Supplementary Information for:

Subrandom Methods for Multidimensional Nonuniform Sampling

Bradley Worley*

Department of Chemistry, University of Nebraska-Lincoln, Lincoln, NE 68588-0304

TABLE OF CONTENTS

Code Listing S-1. Knuth's algorithm for drawing Poisson random deviates.

1. $L \leftarrow e^{-\lambda}$
2. $k \leftarrow 0$
3. $p \leftarrow 1$
4. Repeat:
    a. $k \leftarrow k + 1$
    b. $u \sim U(0, 1)$
    c. $p \leftarrow p \cdot u$
5. Until $p \leq L$.
6. Return $k - 1$ as new Poisson random deviate.

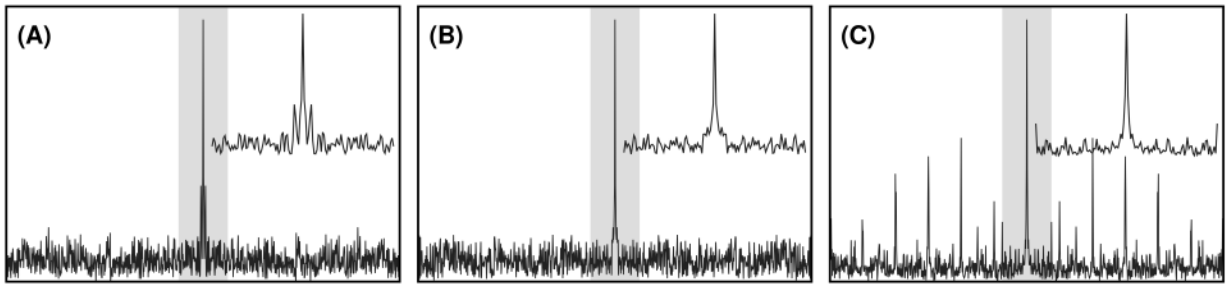

Figure S-1. Comparison of point-spread functions from **(A)** the lowest-PSR pseudorandom schedule, **(B)** the highest-PSR pseudorandom schedule, and **(C)** the subrandom schedule produced without jittering from an exponentially weighted 1024-point Nyquist grid at 10% sampling density. Inset plots indicate the shaded central regions of each point-spread function in order to highlight artifacts near the fundamental. The high coherence of subrandom sampling is readily apparent from panel **(C)**.

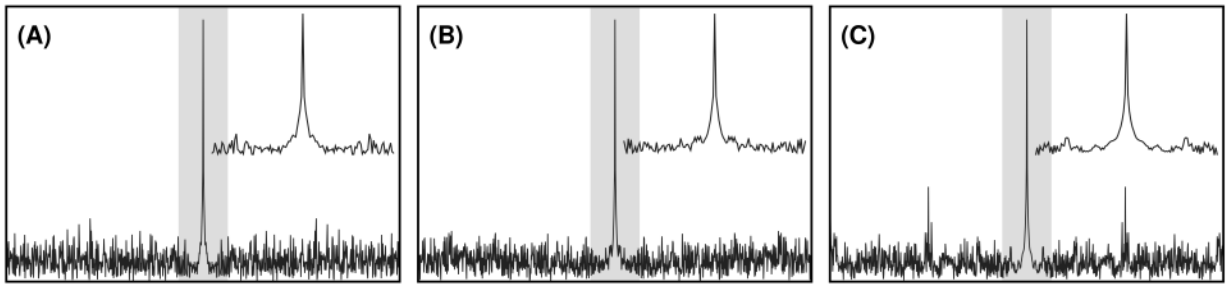

Figure S-2. Comparison of point-spread functions from **(A)** the lowest-PSR pseudorandom Poisson-gap schedule, **(B)** the highest-PSR pseudorandom Poisson-gap schedule, and **(C)** the subrandom Poisson-gap schedule produced from a 1024-point Nyquist grid at 10% sampling density. Inset plots indicate the shaded central regions of each point-spread function in order to highlight artifacts near the fundamental.

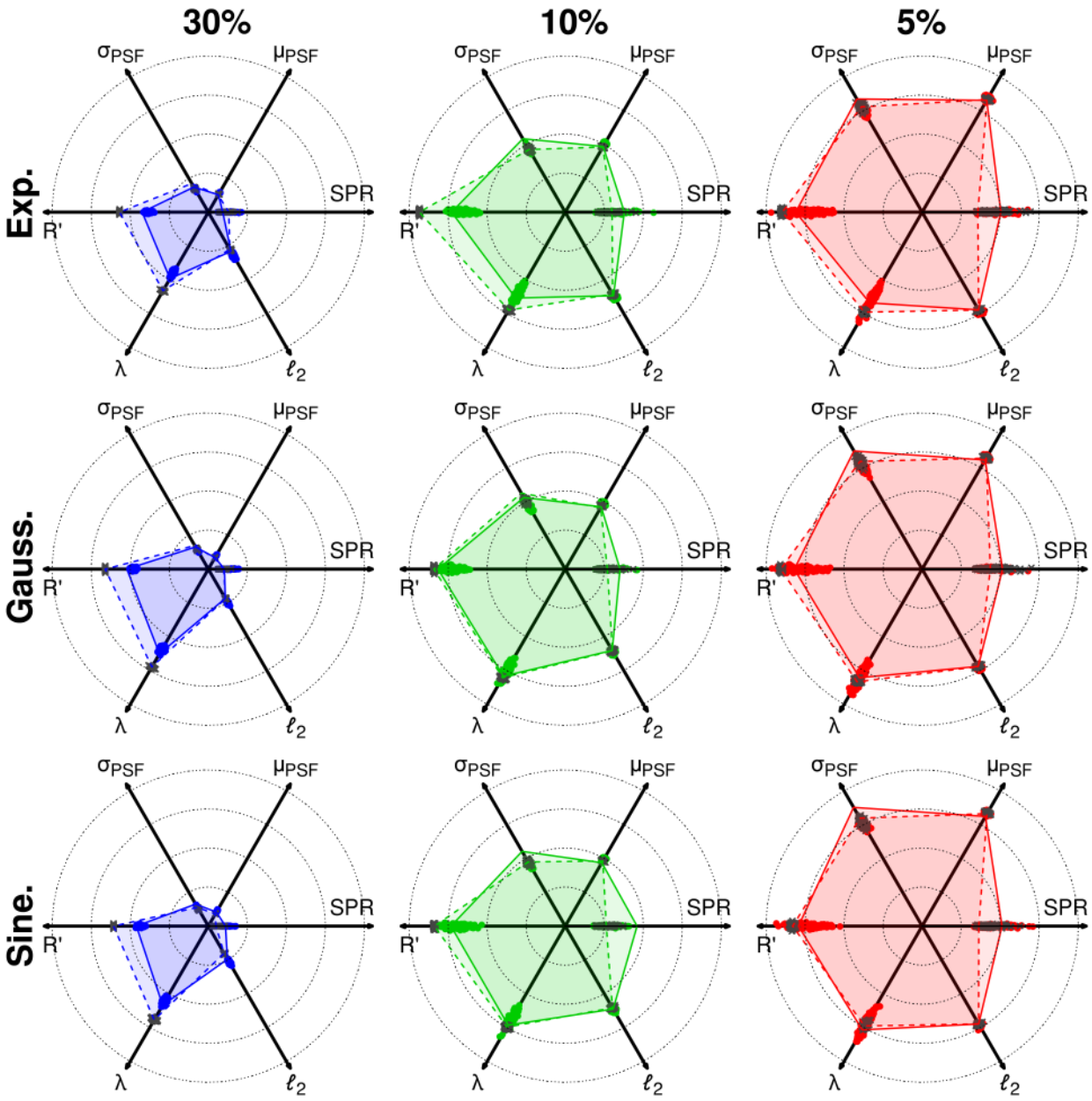

Figure S-3. Radar charts indicating performance metrics for two-dimensional sampling schedules on 64x64-point grids. Metrics from pseudorandom, jittered pseudorandom, subrandom and jittered subrandom schedules are indicated by points, crosses, solid lines and dashed lines, respectively. Displayed ranges for each metric are as follows: SPR: 0.03 – 0.33, μ_{PSF}: 0.01 – 0.07, σ_{PSF}: 0.003 – 0.03, R': 1.4 – 3.2, λ: 0.3 – 1.2, ℓ_2: 0.1 – 0.6. Lower values of each range are placed centrally on the charts, and higher values are placed towards the outer radius.

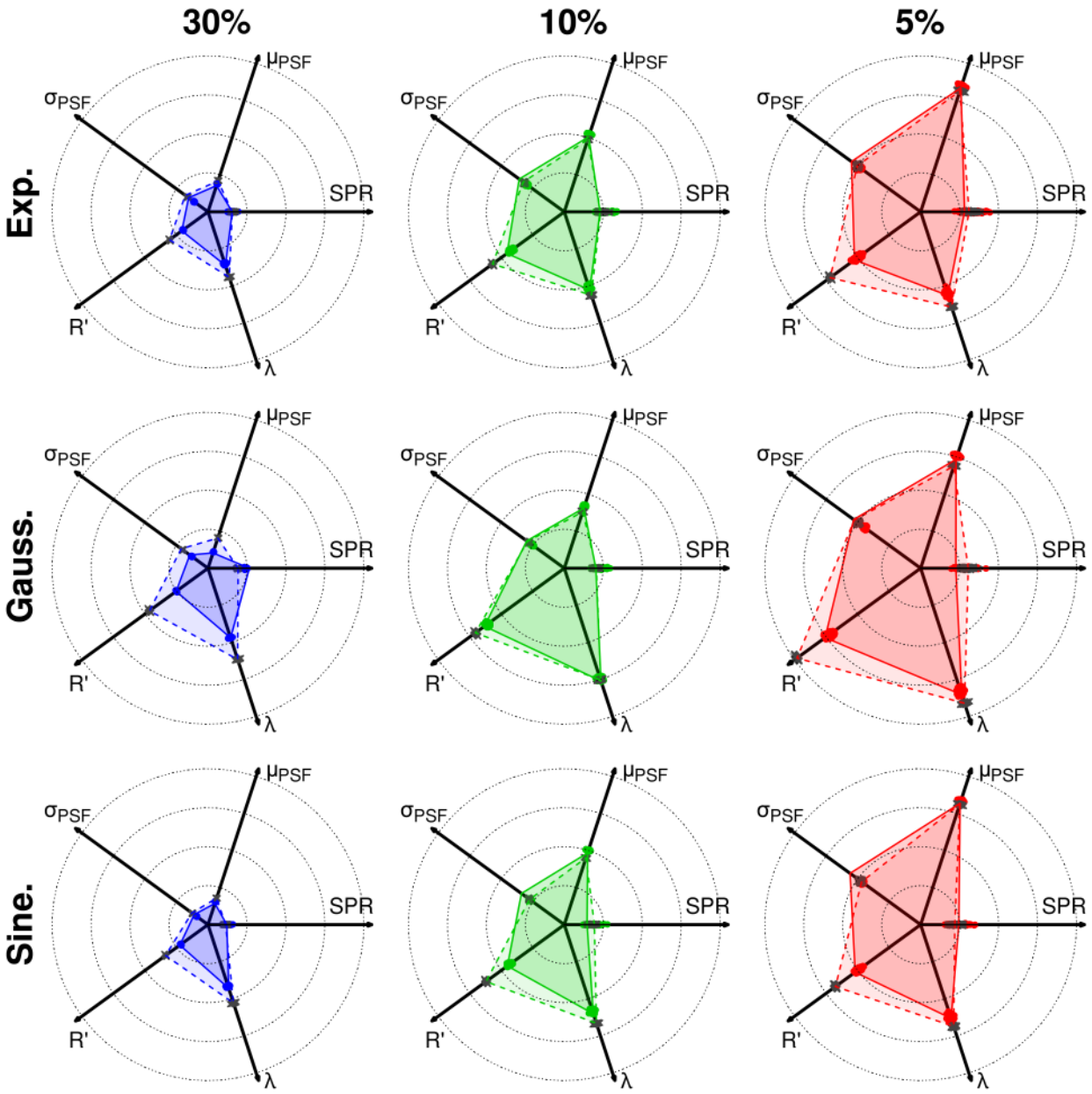

Figure S-4. Radar charts indicating performance metrics for three-dimensional sampling schedules on 32x32x32-point grids. Metrics from pseudorandom, jittered pseudorandom, subrandom and jittered subrandom schedules are indicated by points, crosses, solid lines and dashed lines, respectively. Displayed ranges for each metric are as follows: SPR: 0.02 – 0.25, μ_{PSF}: 0.002 – 0.025, σ_{PSF}: 0.001 – 0.012, R': 1.4 – 6.8, λ: 0.3 – 1.3. Lower values of each range are placed centrally on the charts, and higher values are placed towards the outer radius.

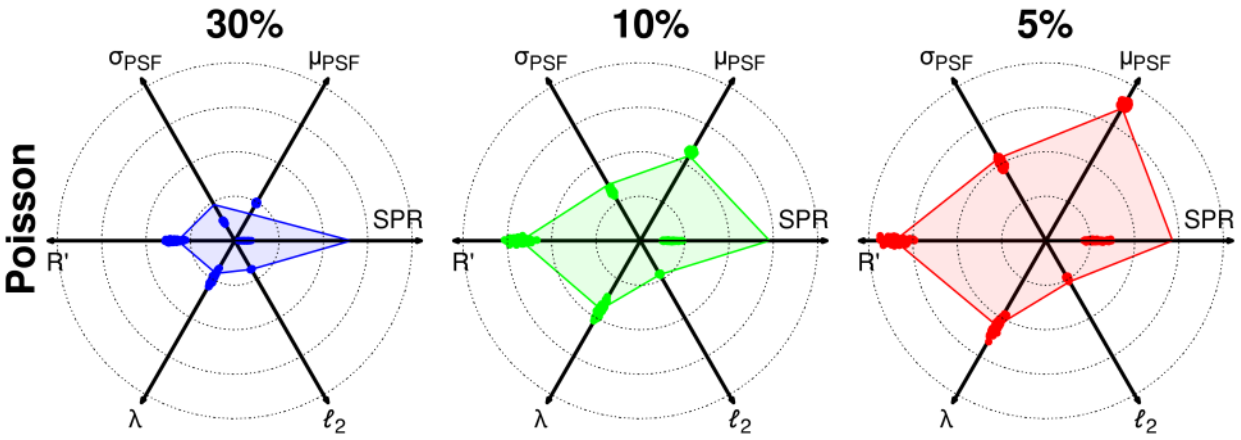

Figure S-5. Radar charts indicating performance metrics for one-dimensional Poisson-gap sampling schedules on 1024-point grids. Metrics from pseudorandom and subrandom schedules are indicated by points and solid lines, respectively. Displayed ranges for each metric are as follows: SPR: 0.08 – 1, μ_{PSF}: 0.01 – 0.13, σ_{PSF}: 0.01 – 0.11, R': 1.1 – 2.2, λ: 0.3 – 1.6, ℓ_2: 0 – 1. Lower values of each range are placed centrally on the charts, and higher values are placed towards the outer radius.

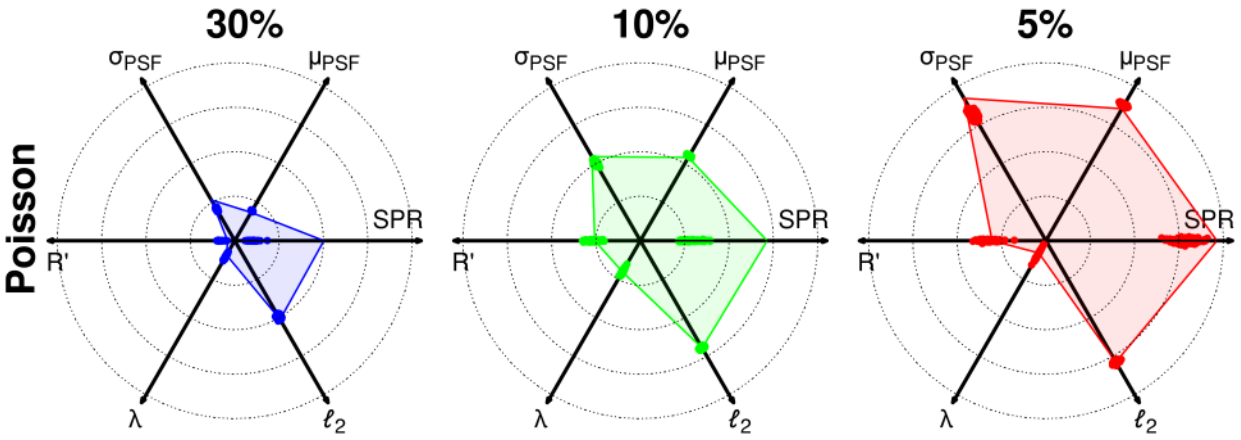

Figure S-6. Radar charts indicating performance metrics for two-dimensional Poisson-gap sampling schedules on 64x64-point grids. Metrics from pseudorandom and subrandom schedules are indicated by points and solid lines, respectively. Displayed ranges for each metric are as follows: SPR: 0.03 – 0.33, μ_{PSF}: 0.01 – 0.07, σ_{PSF}: 0.003 – 0.03, R': 1.4 – 3.2, λ: 0.3 – 1.2, ℓ_2: 0.1 – 0.6. Lower values of each range are placed centrally on the charts, and higher values are placed towards the outer radius.

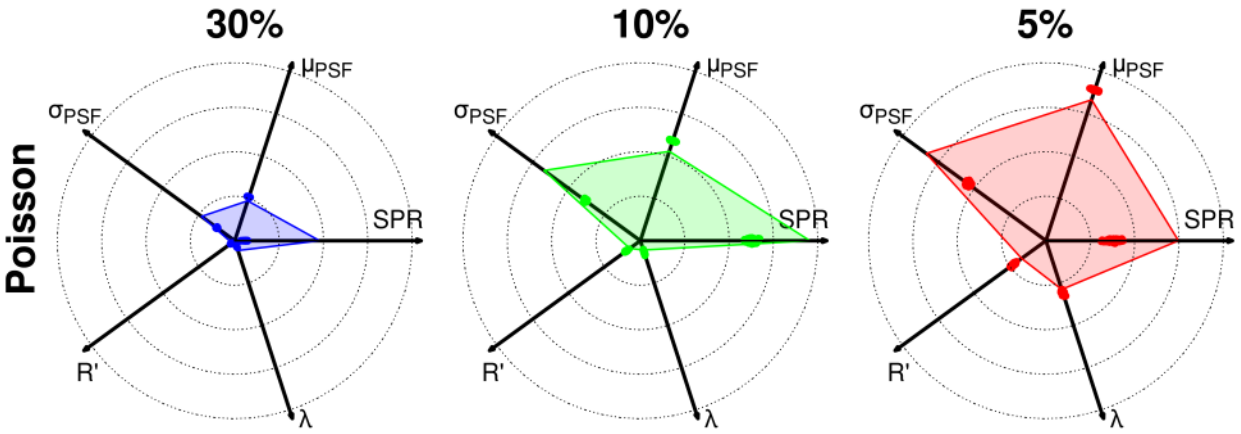

Figure S-7. Radar charts indicating performance metrics for three-dimensional Poisson-gap sampling schedules on 32x32x32-point grids. Metrics from pseudorandom and subrandom schedules are indicated by points and solid lines, respectively. Displayed ranges for each metric are as follows: SPR: 0.02 – 0.25, μ_{PSF}: 0.002 – 0.025, σ_{PSF}: 0.001 – 0.012, R': 1.4 – 6.8, λ: 0.3 – 1.3. Lower values of each range are placed centrally on the charts, and higher values are placed towards the outer radius.

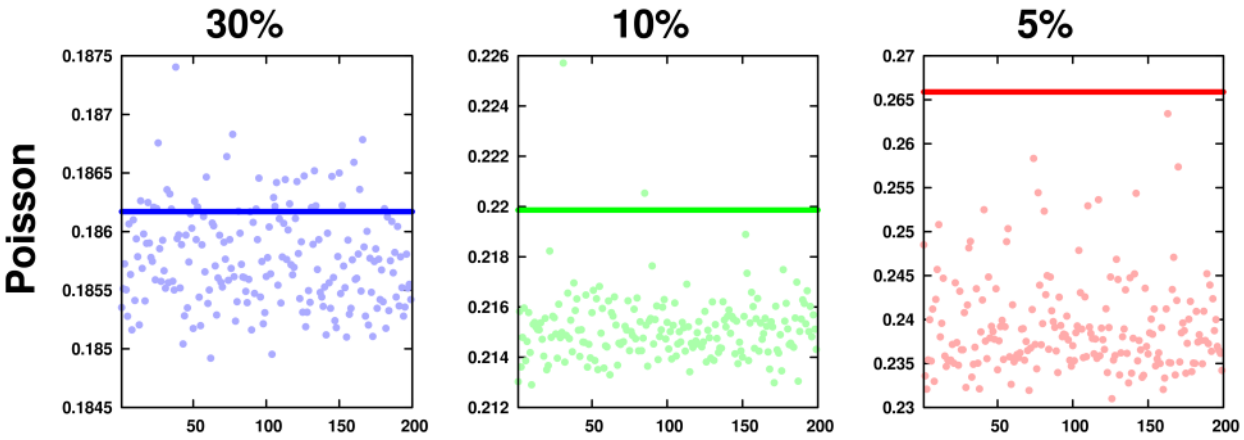

Figure S-8. Expanded view of ℓ_2 reconstruction errors from one-dimensional Poisson-gap sampling methods. Errors from pseudorandom and subrandom schedules are indicated by circles and lines, respectively. In all cases, subrandom sampling performs poorly in comparison to pseudorandom sampling. It should also be noted that one-dimensional Poisson-gap schedules maintain relatively low reconstruction errors, irrespective of sampling density.

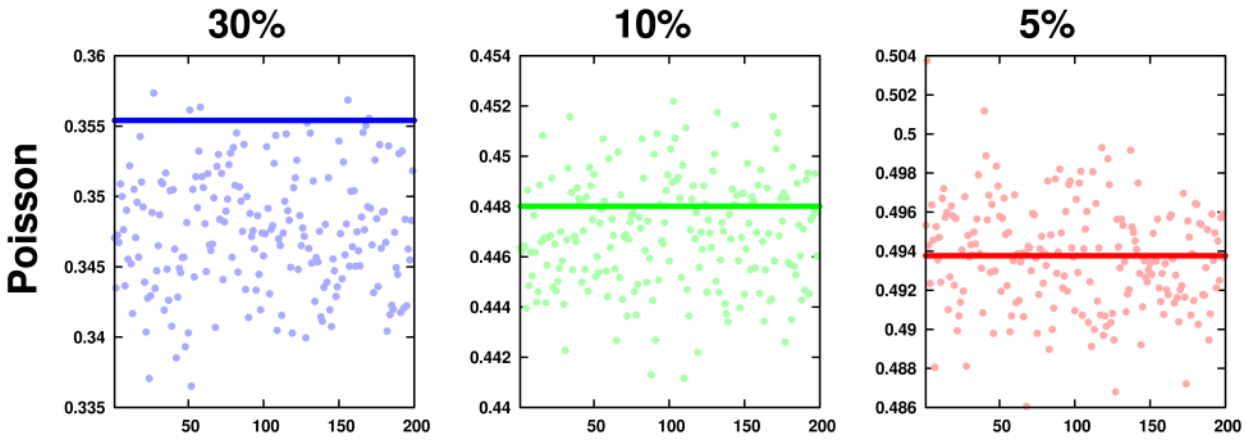

Figure S-9. Expanded view of ℓ_2 reconstruction errors from two-dimensional Poisson-gap sampling methods. Errors from pseudorandom and subrandom schedules are indicated by circles and lines, respectively.

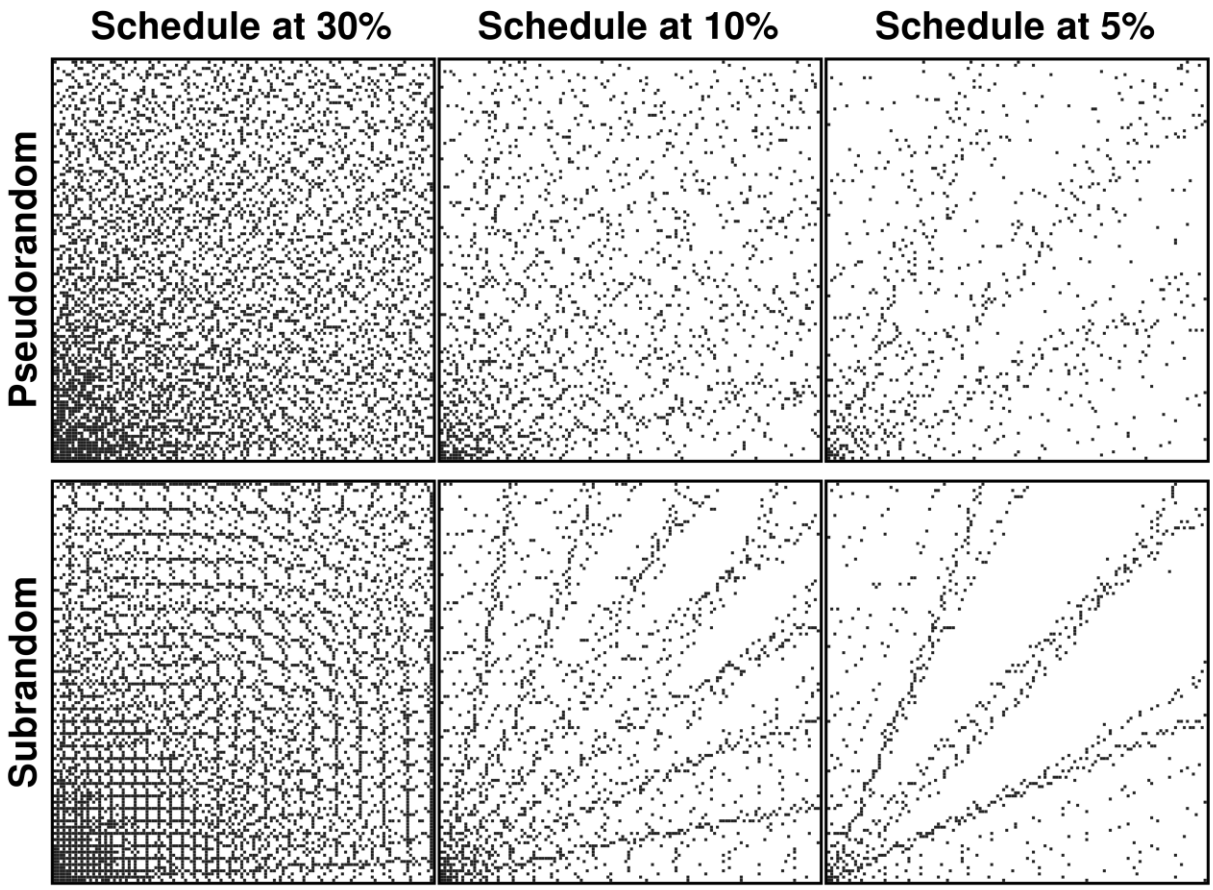

Figure S-10. Illustration of two-dimensional "striped" patterns arising from both pseudorandom and subrandom Poisson-gap sampling methods as global sampling density is decreased.

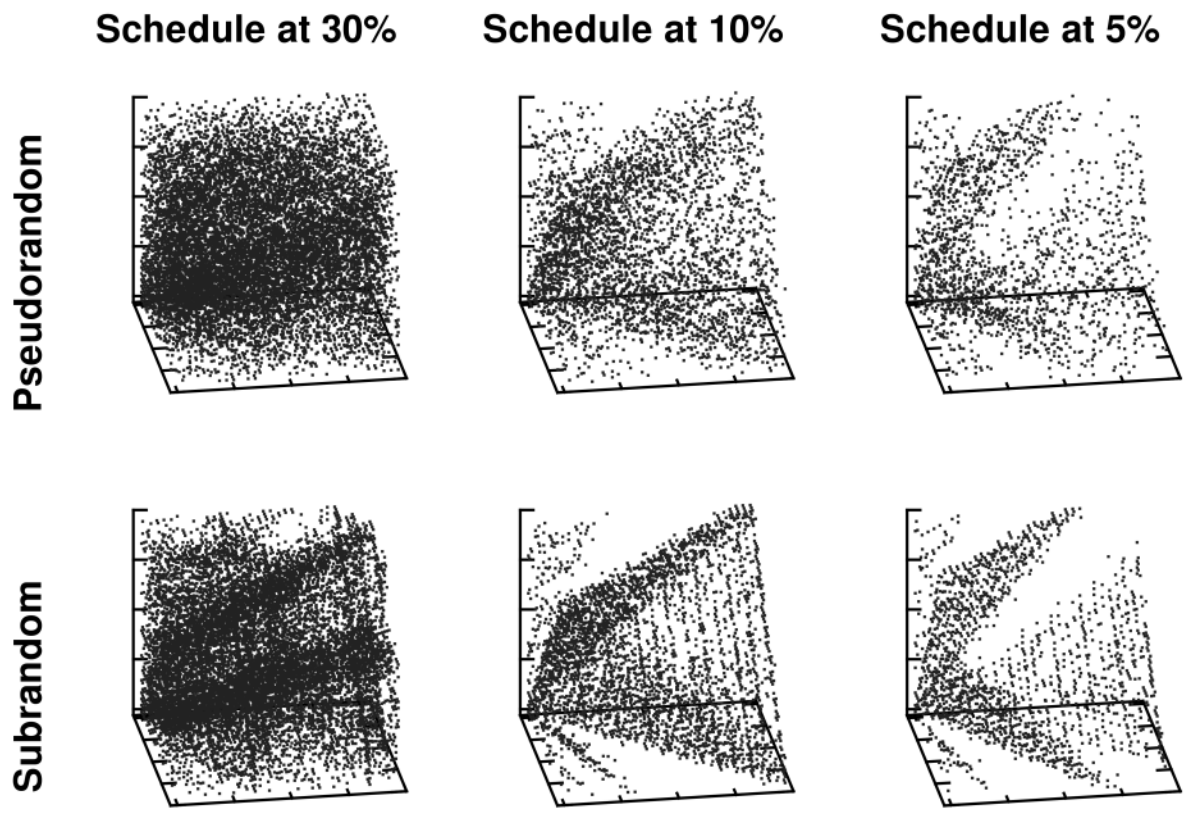

Figure S-11. Illustration in three dimensions of "striped" pattern produced by Poisson-gap sampling using both pseudorandom and subrandom sampling methods.